JVI
Journals.ASM.org

Early Events in Alphavirus Replication Determine the Outcome of Infection

Ilya Frolov, Maryna Akhrymuk, Ivan Akhrymuk, Svetlana Atasheva, and Elena I. Frolova

Department of Microbiology, University of Alabama, Birmingham, Alabama, USA

Alphaviruses are a group of important human and animal pathogens. They efficiently replicate to high titers *in vivo* and in many commonly used cell lines of vertebrate origin. They have also evolved effective means of interfering with development of the innate immune response. Nevertheless, most of the alphaviruses are known to induce a type I interferon (IFN) response *in vivo*. The results of this study demonstrate that the first hours postinfection play a critical role in infection spread and development of the antiviral response. During this window, a balance is struck between virus replication and spread in vertebrate cells and IFN response development. The most important findings are as follows: (i) within the first 2 to 4 h postinfection, alphavirus-infected cells become unable to respond to IFN-β, and this occurs before the virus-induced decrease in STAT1 phosphorylation in response to IFN treatment. (ii) Most importantly, very low, subprotective doses of IFN-β, which do not induce the antiviral response in uninfected cells, have a very strong stimulatory effect on the cells' ability to express type I IFN and activate interferon-stimulated genes during subsequent infection with Sindbis virus (SINV). (iii) Small changes in SINV nsP2 protein affect its ability to inhibit cellular transcription and IFN release. Thus, the balance between type I IFN induction and the ability of the virus to develop further rounds of infection is determined in the first few hours of virus replication, when only low numbers of cells and infectious virus are involved.

Alphaviruses are a group of important human and animal pathogens that are widely distributed all over the world (22, 42). They cause a variety of diseases, with symptoms ranging from mild rash and arthritis to lethal meningoencephalitis (22). One of the critical characteristics of alphaviruses is their efficient replication *in vivo* and in many commonly used cell lines of vertebrate origin (37). Within 6 h, infected cells begin virus release, and within 12 to 16 h postinfection they can produce 10^3 to 10^4 infectious virions per cell and they induce a next round of infection. Moreover, most of the alphaviruses, if not all of them, have developed very efficient means of interfering with induction of the cellular antiviral response (4, 6, 15–17). This leads to downregulation of the antiviral state in the infected cells and ultimately inhibition of the innate immune response, aimed at protection of as-yet-uninfected cells. This virus-specific inhibition of the antiviral and innate responses makes an additional contribution to rapid spread of alphavirus infections.

One of the most efficient means of interference with the innate immune response utilized by alphaviruses is inhibition of cellular transcription. This phenomenon is a characteristic feature of both New World and Old World alphaviruses (17). For the New World alphaviruses, the capsid protein has been found to be a key player in transcription inhibition (2, 15, 17). The tetrameric complex of capsid protein, importin-α/β, and nuclear export receptor CRM1 has been demonstrated to obstruct passage of cellular proteins through the nuclear pore, and this inhibition of nucleocytoplasmic trafficking strongly correlates with the development of transcriptional shutoff (3–5). The Old World alphaviruses employ a different mechanism. Their nsP2 protein, but not capsid protein, is responsible for transcription inhibition (18, 19). A large fraction of nsP2 is transported into the cell nuclei (8, 9, 12, 30), where this protein inhibits function of both the DNA-dependent RNA polymerases I and II (RNA Pol I and II) (16). In cells permissive to viral infection, this leads to robust transcription inhibition within 4 to 6 h postinfection and, thus, prevents activation of antiviral genes.

A number of alphaviruses are also known to induce translational shutoff in infected vertebrate cells (18, 20, 38). Translation inhibition has both protein kinase R (PKR)-dependent and PKR-independent components and is highly beneficial for translation of virus-specific subgenomic RNAs. It appears to be not only a prerequisite of efficient production of viral structural proteins but additionally contributes to downregulation of the antiviral response and to development of cytopathic effect (CPE) (10, 11, 44).

However, as has been demonstrated for other viral infections, alphavirus replication *in vivo* results in expression of type I interferon (IFN) and other cytokines and chemokines (14, 21, 23, 31). Their release leads to protection of the majority of uninfected cells and tissues *in vivo* against new rounds of viral infection until development of the adaptive immune response. Thus, inhibition of the cellular antiviral response *in vivo* is likely to be incomplete. This inability to completely shut off the cellular antiviral defense can be explained by a combination of different factors. One of them relies on the concentration of Old World alphavirus nsP2 and the New World alphavirus capsid proteins, but not their proteolytic activities, in the inhibition of transcription (17). These proteins appear to become fully functional within a few hours postinfection, when their intracellular levels become sufficient for exhibiting the inhibitory functions. Thus, the time period between the beginning of virus replication and induction of virus-specific inhibition of transcription is likely to play an important role in development and spread of infection.

Importantly, the ability of alphaviruses to inhibit cellular mac-

Received 26 December 2011 **Accepted** 9 February 2012
Published ahead of print 15 February 2012
Address correspondence to Elena I. Frolova, efrolova@UAB.edu.

doi:10.1128/JVI.07223-11

romolecular synthesis does not necessarily mean that other, more specific mechanisms of downregulating the antiviral response are not employed. Recent studies have suggested that during alphavirus replication, the cellular antiviral defense system is additionally inactivated by downregulation of STAT1 phosphorylation. STAT1 phosphorylation and its transport to the nucleus are essential to activate transcription of IFN-stimulated genes (ISGs), and alterations of this process affect auto- and paracrine type I IFN signaling (34, 35). This is an important phenomenon and needs further analysis to elucidate its mechanism and biological significance.

In this study, we performed a detailed investigation of the effect of Sindbis virus (SINV) replication on STAT1 function and type I IFN induction in mouse embryonic fibroblasts (MEFs) and of SINV's ability to interfere with the expression of cellular genes. Our data demonstrated that mutations in viral nonstructural genes, particularly in nsP2, make SINV a potent inducer of the host defense in both infected and ultimately in yet-uninfected cells. This makes the SINV mutants incapable of developing a spreading infection. The data also showed that the first 2 to 4 h postinfection are critical in terms of induction of the cell defense mechanisms. If within this time period wild-type (wt) alphavirus replication is established, the subsequent type I IFN treatment does not have a noticeable effect on further virus replication and release. Importantly, pretreatment of cells with very low doses of IFN-β (below 1 U/ml) caused a dramatic increase in type I IFN release during the subsequent infection. This provides a plausible explanation for the very high level of type I IFN detected *in vivo* after infection with SINV. A number of the experiments presented here have also been performed with Venezuelan equine encephalitis virus (VEEV TC-83), a representative member of the New World alphaviruses. The strong correlation of SINV- and VEEV-specific data suggests that the results of this study are applicable to at least some other members of the *Alphavirus* genus.

MATERIALS AND METHODS

Cell cultures. The BHK-21 cells were kindly provided by Paul Olivo (Washington University, St. Louis, MO). The NIH 3T3 cells were obtained from the American Type Culture Collection (Manassas, VA). These cell lines were maintained at 37°C in α-minimum essential medium (α-MEM) supplemented with 10% fetal bovine serum (FBS) and vitamins. The IFN-$\alpha/\beta R^{-/-}$ and wt MEFs were kindly provided by Michael Diamond (Washington University, St. Louis, MO). They were propagated in Dulbecco's MEM supplemented with 10% FBS and nonessential amino acids.

Plasmid constructs. Plasmids carrying SINV and VEEV genomes, pSINV/GFP, pSINV/G/GFP, pSINV/2V/GFP, pSINV/nsP1/GFP, pVEEV/GFP, and pVEEV/Cmut/GFP, have been described elsewhere (5, 12). They encode the cDNA of SINV and VEEV TC-83 genomes with the mutations indicated in the figures and contain an additional subgenomic promoter driving the expression of green fluorescent protein (GFP).

RNA transcriptions and transfections. Plasmids were purified by ultracentrifugation in CsCl gradients. Before transcription reactions, plasmids were linearized using the restriction sites located downstream of the poly(A) sequence of the viral genomes. RNAs were synthesized by SP6 RNA polymerase in the presence of a cap analog under the previously described conditions (29). The yield and integrity of transcripts were analyzed by gel electrophoresis under nondenaturing conditions. RNA concentrations were measured on a FluorChem imager (Alpha Innotech), and transcription reactions were used for electroporation without additional RNA purification. For generating viral stocks, 4 μg of *in vitro*-synthesized RNA was electroporated into BHK-21 cells under previously described conditions (28). Virus titers were determined by plaque assay in BHK-21 cells (27).

IFN-β assay. Concentrations of murine IFN-β in the medium were determined by using the VeriKine Mouse Interferon Beta enzyme-linked immunosorbent assay (ELISA) kit (PBL Interferon Source). In some experiments, concentrations of IFN-α/β in the medium were additionally measured by using a previously described biological assay (12).

Analysis of STAT1 phosphorylation. NIH 3T3 cells were treated with IFN-β at the concentrations indicated in the figures or infected with SINV and VEEV TC-83 variants under the conditions indicated in the figure legends. Cells were harvested at the indicated time points, and equal amounts of protein were analyzed on a 4-to-12% gradient NuPAGE gel (Invitrogen) followed by Western blotting using antibodies against STAT1 (2728; Epitomics), p-STAT1 (812232; BD Biosciences), β-actin (ab6276; Abcam), and alphavirus nsP2 (custom-made monoclonal antibodies) and appropriate infrared dye-labeled secondary antibodies. Images were acquired and processed using a LI-COR imager, and quantitative results were generated using the corresponding software.

Immunofluorescence. For the immunofluorescence studies, NIH 3T3 cells were seeded into Ibidi 8-well μ-slide chambers. They were infected and treated with IFN-β as described in the figure legends, then fixed with methanol and stained with p-STAT1-specific primary and Alexa Fluor 555-labeled secondary antibodies. Images were acquired using the same setting on a Zeiss LSM700 confocal microscope. Quantitative analysis of p-STAT1 accumulation in the cell nuclei was performed using the Zeiss software.

Viral replication analysis. Cells were seeded at a concentration of 5×10^5 cells per well in 6-well Costar plates. After a 4-h-long incubation at 37°C, monolayers were treated with IFN-β and infected with the indicated viruses at the multiplicities of infection (MOIs) described in the corresponding figure legends. At the indicated time points, media samples were harvested and virus titers were determined by a plaque assay on BHK-21 cells as previously described (27). In some of the experiments, the same harvested media were used for measuring the concentration of IFN-β.

RT-qPCR. The total RNA was isolated and used for cDNA synthesis with a QuantiTect reverse transcription (RT) kit (Qiagen). This cDNA was used for quantitative PCR (qPCR) analysis with primers for the following mouse genes: IFN-β (NM_010510), IFIT1 (NM_008331), IFIT3 (NM_010501), GBP3 (NM_018734), ISG15 (NM_015783). The qPCRs were performed using SsoFast EvaGreen supermix (Bio-Rad) in a CFX96 real-time PCR detection system (Bio-Rad). Specificities of the products were tested by measuring their melting temperatures. The data were normalized to the mean threshold cycle (C_T) of 18S RNA in each sample. The fold difference was calculated using the $\Delta\Delta C_T$ method, which uses the mean C_T of the mock sample for normalization. The mRNA of IFN-β was not definitively measured in the mock-infected cells and the samples derived from the cells treated with low doses of IFN-β. Therefore, the data were normalized to the mean C_T for the virus-infected cells. The reactions were performed in triplicates, and the means and the standard deviations were calculated.

RESULTS

Evaluation of STAT1 phosphorylation is a sensitive test for type I IFN detection. In the initial experiments, we intended to analyze the very early events in virus-host cell interactions and first of all to characterize the type I IFN release by the alphavirus-infected cells. At concentrations of type I IFNs below 1 U/ml, standard biological assays and ELISAs for IFN-α/β lack sufficient sensitivity. Thus, we analyzed whether the level of STAT1 phosphorylation could be used for detection of low concentrations of IFN. NIH 3T3 cells were used in this and other experiments as a representative cell line for the IFN-competent cells, as they have no known defects in type I IFN signaling or production. Cells were treated with different concentrations of IFN-β, and relative p-STAT1 levels were

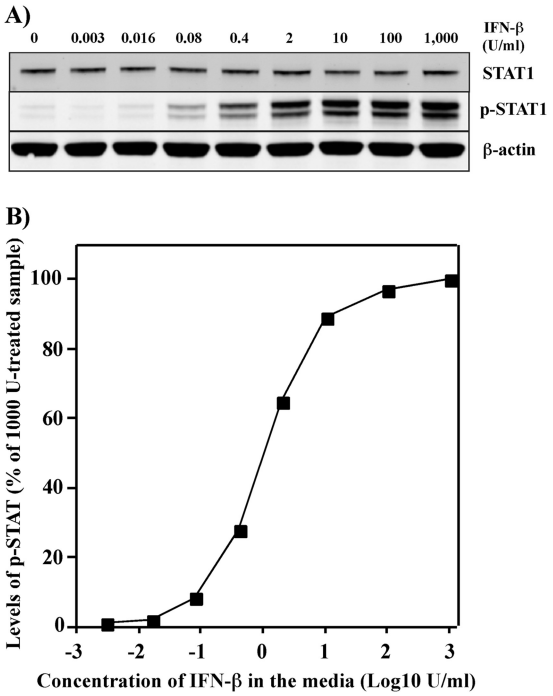

FIG 1 The STAT1 phosphorylation level is a highly sensitive test for detection of IFN-β. (A) NIH 3T3 cells were seeded into 6-well Costar plates at a concentration of 5×10^5 cells per well. After incubation at 37°C for 4 h, cells were treated with IFN-β at the indicated concentrations for 30 min and then harvested and lysed in the protein gel loading buffer. Equal amounts of proteins were separated on a 4-to-12% gradient NuPAGE gel. After protein transfer, the membranes were treated with p-STAT1-, STAT1-, and β-actin-specific antibodies, followed by treatment with infrared dye-labeled secondary antibodies. Membranes were scanned on a LI-COR imager. (B) Results of quantitative p-STAT1 analysis. The signal values for pSTAT1 were normalized to the β-actin signal. The amounts of pSTAT1 are presented as percentages of the amount of p-STAT1 detected in the cells treated with IFN-β at a concentration of 1,000 U/ml.

assessed by Western blotting. The results presented in Fig. 1 clearly demonstrate that the phosphorylated form of STAT1 (p-STAT1), indicative of the IFN treatment, was detectable in the NIH 3T3 cells incubated in the presence of concentrations of IFN-β as low as 0.08 U/ml, reaching saturation at IFN-β concentrations above 100 U/ml. Prior to this and other experiments, the IFN-β stocks were tested for biological activity in the type I IFN bioassay on both NIH 3T3 and L929 cells. One IFN-β unit per milliliter was considered the IFN concentration that protected the cells after 24 h of incubation against subsequent SINV infection, and this value was very similar to the unit of the NIH IFN-α/β standard (data not shown).

The results of this highly reproducible experiment suggest that measurement of STAT1 phosphorylation is a more sensitive assay for detection of IFN-α/β in the medium than standard tests, and it can be used for its sensing at very low concentrations.

Inhibition of cellular transcription is critical for downregulation of the type I IFN response. Next, we assessed whether replication of SINV, a representative member of the Old World alphaviruses, induces type I IFN release. SINV/GFP genomic RNA (Fig. 2A) encoded structural and nonstructural viral proteins derived from the previously designed TE12 variant of the virus (12). The SINV/G/GFP and SINV/2V/GFP genomes had essentially the same sequence but contained a P726G and a G806V mutation in nsP2, respectively. The P726G mutation affects the ability of SINV nsP2 to interfere with cellular RNA polymerase I and II functions (6, 12, 16). The G806V mutation inactivates the cleavage site between nsP2 and nsP3 (33) and, thus, prevents formation of free nsP2 and its migration into the nucleus (19). All of these viruses encoded GFP under the control of the second subgenomic promoter. Expression of GFP allowed us to observe the extent and spread of the infection in the cell monolayers.

In repeated experiments, NIH 3T3 cells infected with wt nsP2-encoding SINV/GFP reproducibly demonstrated no detectable level of STAT1 phosphorylation up to 16 h postinfection (Fig. 2B and C). However, two other SINV variants, SINV/G/GFP and SINV/2V/GFP, containing mutations in nsP2 and, thus, having altered abilities to interfere with cellular transcription (18), demonstrated a strong increase in p-STAT1 levels within the first 4 h postinfection (Fig. 2B and C). This was a strong indication that the ability to interfere with cellular transcription plays a critical role in SINV's ability to inhibit the type I IFN production and corresponding signaling pathway. Importantly, based on our previously published data (12, 18), the distinguishing characteristic of the SINV/G/GFP mutant is an inability to cause both transcriptional and translational shutoffs. However, the SINV/2V/GFP variant remains capable of inducing translation inhibition as efficiently as does the wt virus, while being unable to downregulate transcription of cellular genes. The inability of this cleavage mutant to interfere with type I IFN induction indicates that transcriptional, but not translational, shutoff is a key component in SINV-specific countermeasures against the antiviral response.

To additionally confirm the importance of transcription inhibition in alphavirus replication and to gain insight as to whether or not it is a common feature of alphaviruses, we performed a similar experiment with two VEEV TC-83 derivatives, VEEV/GFP and VEEV/Cmut/GFP (Fig. 2D). VEEV/GFP encodes a wt capsid protein, exhibiting the natural transcription inhibitory functions. The VEEV/Cmut/GFP mutant contained the previously characterized mutations in the capsid gene (5). These mutations made capsid protein incapable of inhibiting nucleocytoplasmic trafficking and cellular transcription (3). In good correlation with our previous data concerning IFN-β induction by VEEV variants (5), the wt capsid protein-expressing virus induced only a low level of type I IFN, which was detected by STAT1 phosphorylation at very late times postinfection (Fig. 2E and F), after CPE development. The VEEV/Cmut/GFP mutant-infected cells, in contrast, demonstrated STAT1 phosphorylation at 4 h postinfection (Fig. 2E and F), suggestive of early type I IFN release.

Taken together, these data demonstrate that inhibition of transcription of cellular RNAs by genetically diverse alphaviruses plays a critical role in inhibition of cellular signaling, the hallmark of which is expression of type I IFN.

Mutations in nsP2 have a strong negative effect on SINV's ability to spread in NIH 3T3 cells. The inability of SINV nsP2 mutants to inhibit cellular transcription suggested that even small alterations in processing or integrity of this protein might have deleterious effects on SINV's ability to spread in cells competent in type I IFN signaling and production. To test this possibility, in the next experiment we used a wt nsP2-encoding SINV/GFP, the above-described SINV/2V/GFP and SINV/G/GFP, and SIN/nsP1/GFP (Fig. 3A). The latter virus contained the previously described mutation I538T in the nsP1-coding sequence, which alters pro-

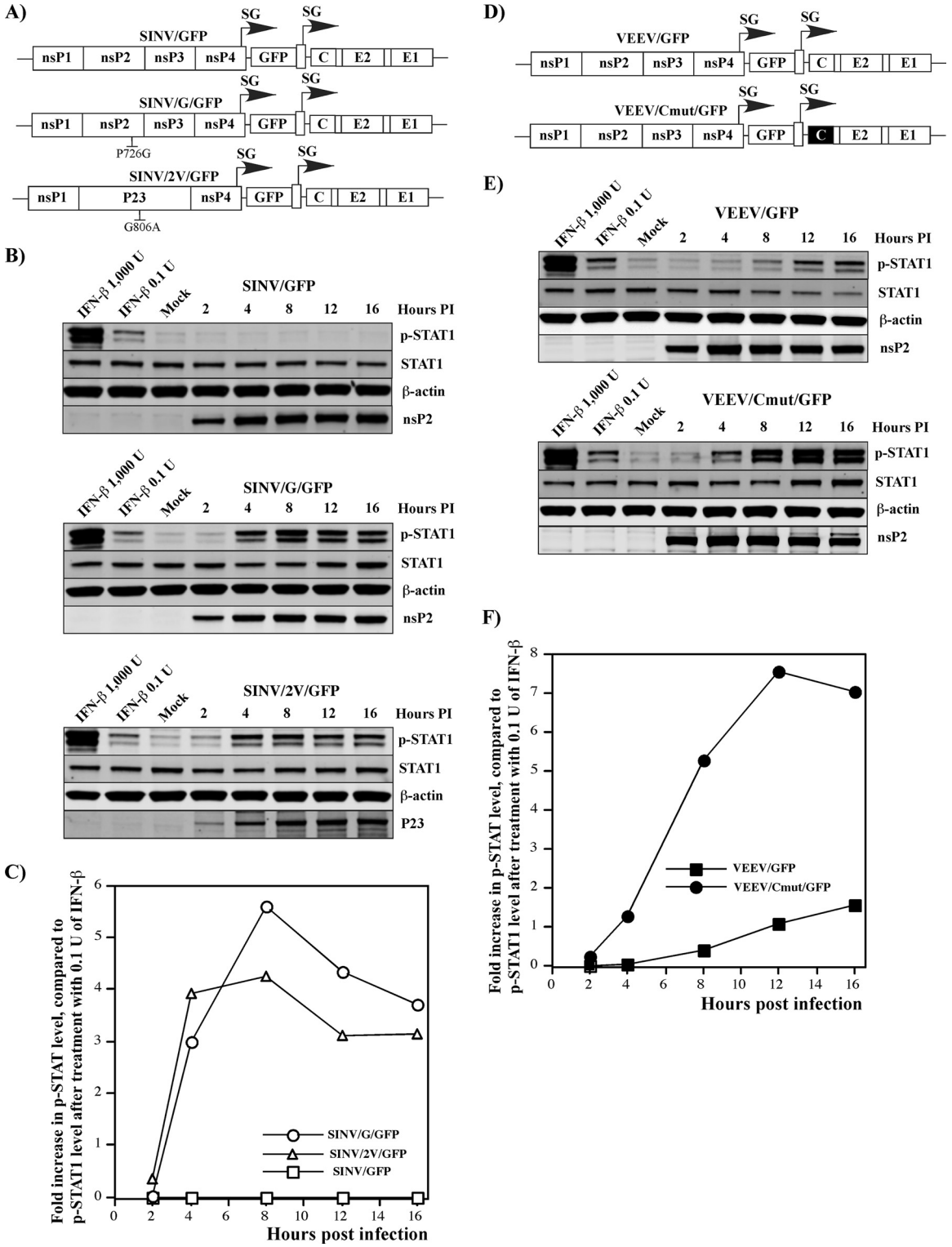

FIG 2 Alterations in SINV nsP2 or VEEV capsid proteins strongly increase type I IFN release by infected cells. (A) Schematic representation of the genomes of SINV variants containing mutations in the nsP2 gene. (B) Results of the analysis of STAT1 phosphorylation in cells infected with SINV variants. NIH 3T3 cells were seeded into 6-well Costar plates at a concentration of 5×10^5 cells per well. They were infected with the indicated viruses at an MOI of 20 PFU/cell and harvested at the indicated time points. Equal amounts of cell lysates were analyzed by PAGE followed by Western blotting using p-STAT1-, STAT1-, nsP2-, and β-actin-specific antibodies and infrared dye-labeled secondary antibodies. Membranes were scanned on a LI-COR imager. (C) Results of quantitative analysis of STAT1 phosphorylation. The signal values for p-STAT1 were normalized to the β-actin signal. The data are presented as the fold increase relative to the amount of p-STAT1 detected in cells treated for 30 min with 0.1 U/ml of IFN-β. (D) Schematic representation of the genomes of VEEV variants used in this study. VEEV/GFP encodes wt capsid protein, and VEEV/Cmut/GFP encodes capsid protein with previously described mutations (5). (E) Results of the analysis of

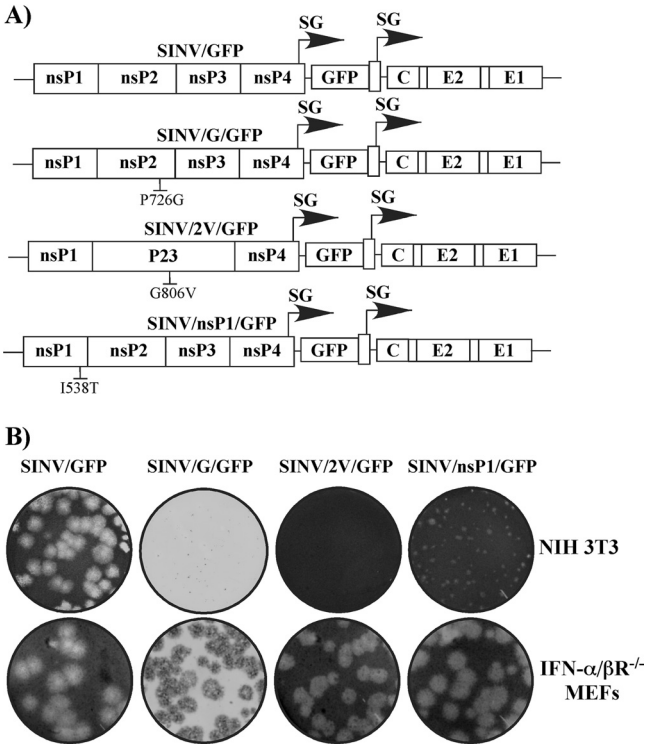

FIG 3 Alterations of nsP2 sequence or ns polyprotein processing affect SINV spread in IFN-competent cells, but not in IFN-$\alpha/\beta R^{-/-}$ MEFs. (A) Schematic representation of SINV mutants used in the experiment. Mutations in nsP2 and nsP1 proteins are indicated. (B) SINV variants encoding the indicated mutations were used in a plaque assay performed on both NIH 3T3 cells and immortalized IFN-$\alpha/\beta R^{-/-}$ MEFs. Plaques were stained with crystal violet at 48 h postinfection. Due to the noncytopathic phenotype of SINV/G/GFP, foci of GFP-positive cells were directly imaged on a Typhoon Imager at 48 h postinfection, after fixation with 4% paraformaldehyde.

cessing rates of the ns polyprotein (24). All of these viruses were used to perform plaque assays on both IFN-competent NIH 3T3 cells and IFN-$\alpha/\beta R^{-/-}$ MEFs (Fig. 3B). As expected, SINV/GFP formed large plaques in both cell lines. The nsP2 cleavage mutants SINV/2V/GFP and SINV/nsP1/GFP, both bearing defects in ns polyprotein processing, readily formed large plaques on the IFN-$\alpha/\beta R^{-/-}$ MEFs but could only produce plaques of a small size (SINV/nsP1/GFP) or pinpoint (SINV/2V/GFP) on the type I IFN-competent NIH 3T3 cells (Fig. 3B). Due to its noncytopathic phenotype, SINV/G/GFP did not cause plaque formation on either cell line but produced very large foci of GFP-positive cells in IFN-$\alpha/\beta R^{-/-}$ MEFs and pinpoint foci of GFP-positive cells in the NIH 3T3 cells (Fig. 3B). SINV/2V/GFP mutants did not form foci of GFP-expressing cells on the NIH 3T3 cells (data not shown), because by 2 days postinfection a few initially infected cells were dead, likely due to translation inhibition, and others remained uninfected.

Taken together, these data suggested that SINV mutants with an altered nsP2 amino acid sequence or altered ns polyprotein processing are able to induce type I IFN, which locally protects IFN-competent cells near those already infected against the next rounds of infection.

Replication of alphaviruses disrupts STAT1 phosphorylation in NIH 3T3 cells only at late times postinfection. The data described in the previous sections suggested that in NIH 3T3 cells, replication of SINV-expressing wt nsP2 did not cause STAT1 phosphorylation, indicative of IFN release and autocrine signaling. However, the lack of phosphorylation could be explained by either an inhibition of IFN-α/β release or by virus-specific changes in the STAT1 phosphorylation process, or both. Moreover, recently published data suggested that alphavirus replication indeed strongly inhibits STAT1 phosphorylation and, thus, prevents activation of IFN signaling pathways (7, 34, 35). The majority of these previously published experiments were performed on Vero cells, which are IFN sensitive but defective in type I IFN expression. Additionally, the data were taken at late times postinfection, when infected cells already demonstrate strong changes in morphology and biological functions and efficiently produce infectious virus. Therefore, to eliminate the Vero cell-specific effects, which could account for a lack of STAT1 phosphorylation during SINV replication, in the next experiments we infected the NIH 3T3 cells with SINV/GFP and treated them for 30 min with IFN-β at a concentration of 500 U/ml at various time points postinfection. Levels of STAT1 phosphorylation were then assessed by Western blotting. Replication of SINV expressing wt nsP2 resulted in a detectable reduction of STAT1 phosphorylation. By 6 h postinfection, infected cells responded to IFN-β treatment with an almost-3-fold lower phosphorylation level of STAT1 than did uninfected cells (Fig. 4). However, even at 8 h postinfection, p-STAT1 was readily detectable after IFN-β treatment.

VEEV infection in the NIH 3T3 cells had an even smaller effect on phosphorylation of STAT1 in response to IFN-β treatment. At 8 h postinfection, addition of IFN-β caused p-STAT1 to accumulate to 60% of the level found in uninfected cells (Fig. 4). Thus, the data demonstrates that replication of two alphaviruses, VEEV and SINV, alters STAT1 phosphorylation in response to type I IFN treatment but does not prevent p-STAT1 from accumulating to readily detectable levels. It seems highly unlikely, at least at early times postinfection (2 to 4 h postinfection), that a lack of p-STAT1 in SINV- and VEEV TC-83-infected NIH 3T3 cells, described in the previous section, was a result of strong, virus-specific changes in the STAT1 phosphorylation pathway.

In the next round of experiments, we tested whether replication of SINV/GFP inhibits translocation of p-STAT1 to the nucleus. NIH 3T3 cells were infected for different durations and then treated with IFN-β for 30 min. The data presented in Fig. 5A and B demonstrate that until 8 h postinfection, p-STAT1 could be readily detected in cell nuclei. The concentration of p-STAT1 in the nuclei following IFN treatment decreased with time after

STAT1 phosphorylation in cells infected with the indicated VEEV variants. NIH 3T3 cells were seeded into 6-well Costar plates at a concentration of 5×10^5 cells per well. They were infected with VEEV/GFP or VEEV/Cmut/GFP at an MOI of 20 PFU/cell and harvested at the indicated time points. Equal amounts of cell lysates were analyzed on 4-to-12% gradient NuPAGE gels, followed by Western blotting using p-STAT1-, STAT1-, nsP2-, and β-actin-specific antibodies and infrared dye-labeled secondary antibodies. Membranes were scanned on a LI-COR imager. (F) Results of quantitative analysis of STAT1 phosphorylation in VEEV-infected cells. The signal values for p-STAT1 were normalized to the β-actin signal. The data are presented as the fold increase relative to the amount of p-STAT1 detected in the cells treated for 30 min with 0.1 U/ml of IFN-β.

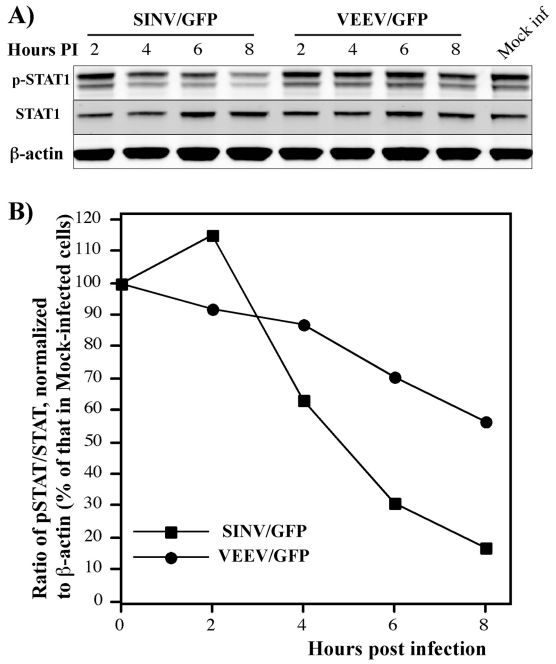

FIG 4 Alphavirus-infected NIH 3T3 cells continue to respond to IFN-β treatment by STAT1 phosphorylation. (A) NIH 3T3 cells were infected with SINV/GFP or VEEV/GFP at an MOI of 20 PFU/cell, and at the indicated times postinfection cells were treated with 500 U/ml of mouse IFN-β for 30 min. Then, cells were harvested, and equal amounts of lysates were analyzed by electrophoresis on a 4-to-12% gradient NuPAGE gel, followed by Western blotting using p-STAT1-, STAT1-, and β-actin-specific antibodies and infrared dye-labeled secondary antibodies. Membranes were scanned on a LI-COR imager. (B) Ratios of p-STAT1/STAT1 signals at different times postinfection. The results are normalized to the ratio determined in the mock-infected cells treated with IFN-β at the same concentration.

SINV/GFP infection. However, this change in nuclear accumulation appeared to correlate with the efficiency of STAT1 phosphorylation (Fig. 4) rather than with potential changes in its nuclear transport. Nevertheless, small changes in transport rates cannot be ruled out. Importantly, significant (2- to 3-fold) changes in p-STAT1 accumulation in the nuclei were found only beyond 4 h postinfection, a point after which virus replication has already become resistant to IFN-β treatment (see below).

SINV replication becomes resistant to IFN-β treatment at very early times postinfection. The data described above indicated that until 4 to 6 h postinfection, SINV replication does not have a deleterious effect on the ability of STAT1 to be phosphorylated in response to IFN-β treatment. p-STAT1 was also capable of translocation into cell nuclei. However, by 6 to 8 h postinfection, changes in the STAT1 phosphorylation level and its accumulation in the nuclei were noticeable (Fig. 5). Their possible biological significance and the importance of the remaining p-STAT1 transport required evaluation. Therefore, we next assessed the ability of cells to mount the antiviral state and interfere with virus replication in response to IFN-β treatment at different times postinfection.

NIH 3T3 cells were infected with SINV/GFP or SINV/G/GFP at an MOI of 20 PFU/cell. IFN treatment was started at different times before or after the infection (Fig. 6). Virus titers were measured at 20 h postinfection. In order to detect possible differences in the inhibitory effect of IFN-β on different viruses in these experiments, it was intentionally used at lower concentration (50 U/ml) than in others.

The IFN-β treatment had a strong negative effect on replication of SINV/GFP only when it was applied either before the infection or within the first 1 to 2 h postinfection. By 3 to 4 h postinfection, almost no effect of IFN-β on virus replication was detected, and cells released infectious virus to essentially the same titers as the mock-treated cells. The SINV/G/GFP variant containing an attenuating mutation in the nsP2 gene demonstrated essentially the same dependence of replication on the start time of IFN-β treatment (Fig. 6B). However, it should be noted that this noncytopathic mutant is unable to establish persistent infection in IFN-competent cells (5, 12). Its clearance within 7 to 8 days postinfection was shown to be strictly dependent on autocrine type I IFN signaling (5, 12), suggesting the importance of the long-term, IFN-dependent antiviral response in inhibition of replication of SINV nsP2 mutants.

Very similar results were obtained in experiments with VEEV/GFP and VEEV/Cmut/GFP viruses (Fig. 6B and data not shown): after 3 h postinfection, the IFN-β effect on virus replication was negligible. In agreement with previously published data (43), replication of VEEV variants was noticeably more resistant to IFN-β treatment (Fig. 6B). It replicated to relatively high titers when the treatment was performed even at 0 to 1 h postinfection.

These experiments allowed us to draw some conclusions. First, IFN-β treatment had a very small effect or no effect at all on SINV replication if infection had already been established in the cells. Three hours post-SINV/GFP infection, NIH 3T3 cells were no longer able to interfere with virus replication, even if IFN-β was present in the medium. Second, this phenomenon was not limited to SINV. By 2 to 3 h postinfection, replication of the distantly related alphavirus VEEV TC-83 was also resistant to type I IFN treatment. Third, the ability of SINV to replicate in the presence of IFN-β after 3 h postinfection did not depend on its nsP2-mediated nuclear function(s). The SINV/G/GFP mutant, which is incapable of interfering with cellular transcription, can produce infectious virus in the presence of IFN-β if virus replication has been already established. Last, it is highly unlikely that changes in STAT1 phosphorylation, which occur by 6 to 8 h postinfection with SINV, have a strong positive effect on virus replication. By this time, replication cannot be significantly altered by IFN-β treatment. More likely, the reduction in STAT1 phosphorylation in SINV/GFP-infected cells is determined by changes in concentrations of proteins involved in IFN signaling, resulting from global inhibition of macromolecular synthesis.

Priming with low, subprotective doses of IFN-β strongly stimulates IFN-β release and activation of ISGs. The results of this study and previous work on SINV-host cell interactions produced some ambiguity. wt SINV replication is able to completely inhibit activation of cellular IFN-stimulated genes and the type I IFN-specific genes themselves. Nevertheless, SINV replication *in vivo* does induce IFN production, and during the infection, type I IFN is detected in the blood of infected animals at relatively high concentrations (12, 26, 39, 40). To provide a plausible explanation for this discrepancy, we made a simple assumption: in cells less permissive to SINV infection, lower levels of nsP2 are expressed. As a result, the antiviral response is not rapidly inhibited, and such cells are capable of producing low levels of type I IFN. The level of released IFN is insufficient for protecting as-yet-uninfected cells

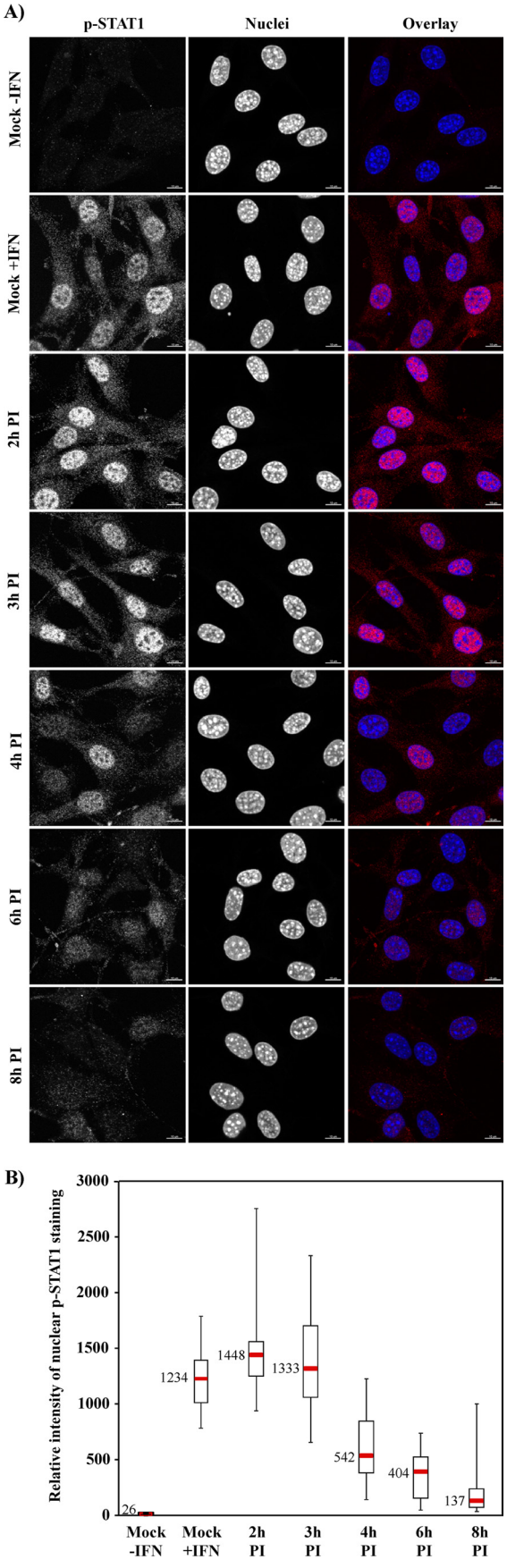

but primes these cells to promote higher levels of IFN expression upon subsequent infection with SINV.

Indeed, we readily detected low levels of IFN-β in the media of murine bone marrow cells and of dendritic cells infected with SINV/GFP (data not shown), suggesting that IFN priming might be an important phenomenon during the development of a spreading infection.

To further test this hypothesis, we treated NIH 3T3 cells with low, subprotective doses of IFN-β for 2 h. These monolayers were then used for a virus plaque assay. The results presented in Fig. 7 demonstrate that concentrations of IFN-β as low as 0.1 and 0.2 U/ml did not protect cells against primary infection, and SINV/GFP formed small, GFP-positive foci on the pretreated cells as efficiently as it formed plaques on the nontreated NIH 3T3 cells. However, this treatment efficiently inhibited the infection spread, most likely due to higher local accumulation of IFN caused by agarose cover. Similar inhibition of plaque development was detected in the experiments with VEEV/GFP, suggesting that the priming effect can be detected for at least some other alphaviruses (Fig. 7).

In another set of experiments, NIH 3T3 cells were treated with 0.2 U/ml of IFN-β for 2 h and then infected with different doses of SINV/GFP (Fig. 8). At 20 h postinfection, we analyzed the concentration of released virus (Fig. 8A), accumulation of IFN-β in the medium (Fig. 8B), and CPE development (Fig. 8C). The data were compared to those obtained with mock-treated, infected cells. As expected, the mock-treated cells did not respond by IFN-β release at any of the MOIs used; the detected values were at the background level. They also produced virus to essentially the same titers, regardless of the MOI. However, the IFN-pretreated cells produced less virus (Fig. 8A) and dramatically higher levels of IFN-β, which were readily detected by ELISA. The levels of both virus and IFN release, and also CPE development, were in good correlation with the used MOIs. This was an indication that only primary infected cells were responsible for the IFN response, which in turn prevented further virus spread in the cultures infected at low MOIs. In multiple reproducible experiments, very high MOIs (20 to 200 PFU/cell) of SINV/GFP induced lower levels of IFN-β in pretreated cultures, indicating that interference with the IFN response can occur, but its efficiency likely depends on how fast cells succumb to infection.

The detected dependence of the IFN response on the MOI, in addition to the results of previously published experiments (25), also left the possibility that the IFN response is induced by incoming virus particles, but not by virus replication. To rule out this possibility, NIH 3T3 cells were infected with the same numbers of UV-inactivated SINV particles, as indicated in Fig. 8A. No IFN induction was detected at any MOI in the IFN-pretreated or mock-treated cells (data not shown).

FIG 5 SINV infection affects accumulation of p-STAT1 in cell nuclei at late times postinfection. (A) NIH 3T3 cells were infected with SINV/GFP at an MOI of 20 PFU/cell in Ibidi 8-well μ-slide chambers. By 2 h postinfection, all of the cells demonstrated GFP expression, indicative of virus replication. At the indicated times postinfection, cells were treated for 30 min with IFN-β at a concentration of 500 U/ml. Then, cells were fixed and stained with p-STAT1-specific primary and Alexa Fluor 555-labeled secondary antibodies. For all of the samples, images were acquired using the same setting on a Zeiss LSM700 confocal microscope. (B) Quantitative analysis of p-STAT1 accumulation in the cell nuclei was performed using the Zeiss software, and 40 cells in randomly selected fields were used for every time point.

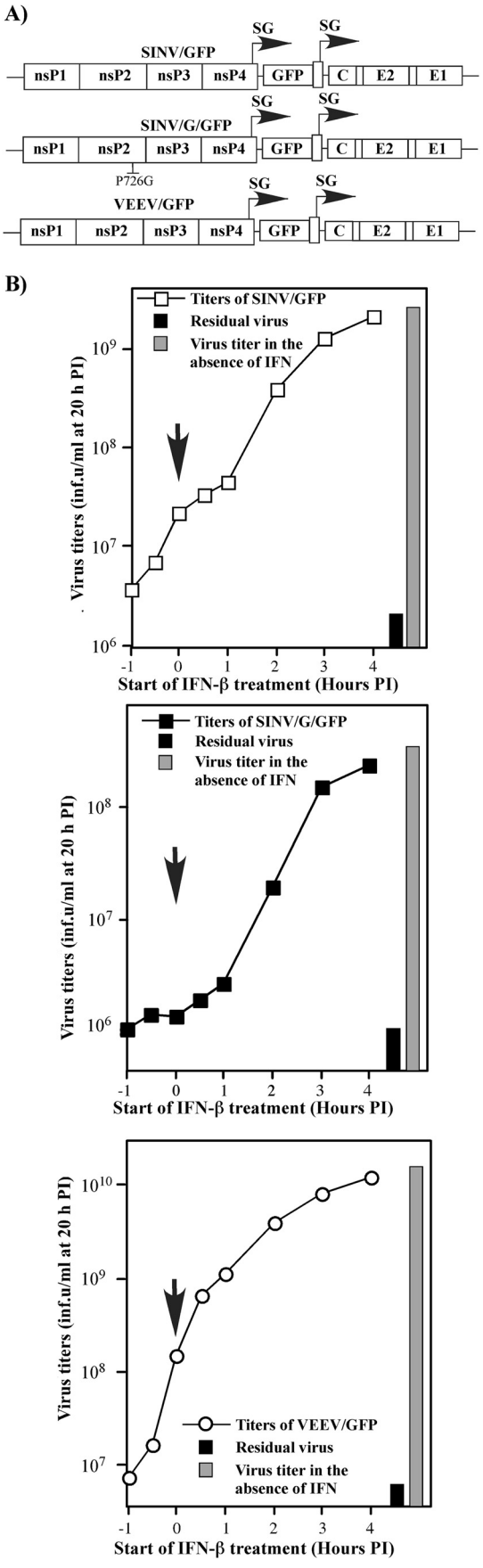

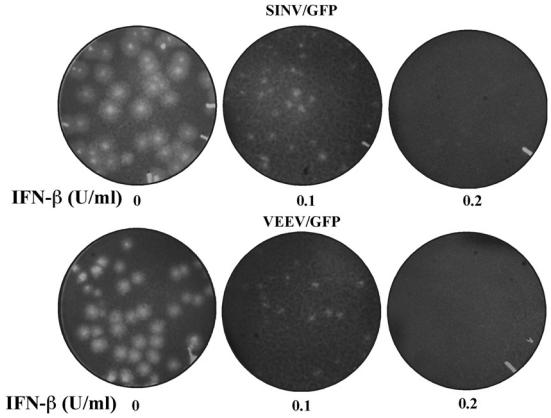

FIG 7 Pretreatment of NIH 3T3 cells with low, subprotective doses of IFN-β strongly affects infection spread. NIH 3T3 cells were seeded into 6-well Costar plates at a concentration of 5×10^5 cells per well. Prior to infection, IFN-β was added to some plates to concentrations of 0.1 or 0.2 U/ml. After 2 h of incubation, SINV/GFP and VEEV/GFP were titrated on IFN-β-pretreated and mock-treated cells. The agarose cover contained IFN-β at the indicated concentrations. Presented wells were infected with exactly the same doses of SINV/GFP or VEEV/GFP.

To rule out the possibility that the detected increase in the antiviral response is specific to IFN-β, we also tested activation of some other cellular genes that we previously found to be efficiently induced by VEEV/Cmut/GFP replication (5). qPCR analysis was performed on RNA samples isolated from (i) naïve NIH 3T3 cells, (ii) cells treated with 0.2 U/ml of IFN-β for 20 h, (iii) cells infected with SINV/GFP at an MOI of 2 PFU/cell for 20 h, and (iv) cells pretreated with 0.2 U/ml of IFN-β for 2 h and then infected with SINV/GFP at an MOI of 2 PFU/cell for 20 h. We tested the difference in concentrations of mRNAs specific to IFN-β, IFIT1, IFIT3, GBP3, and ISG15. All of the tested RNA templates were found at concentrations orders of magnitude higher in the samples isolated from cells pretreated with IFN-β and then infected with SINV than in the samples isolated from cells that were simply IFN-β treated or those mock treated and infected (Fig. 9). A low dose of IFN-β or SINV alone was insufficient to cause the increase in expression of the ISGs tested.

Taken together, the data strongly suggested that brief pretreatment of NIH 3T3 cells with low, subprotective doses of IFN-β before subsequent SINV infection has a strong stimulatory effect on type I IFN production and activation of other antiviral genes. The higher level of IFN release is determined not by SINV particles entering the cell, but by intracellular virus replication. This phenomenon of amplified IFN release is particularly noticeable when

FIG 6 Alphavirus replication rapidly becomes resistant to IFN-β treatment. (A) Schematic representation of the genomes of recombinant viruses used in this study. (B) Analysis of virus replication in cells treated with IFN-β at different times postinfection or prior to infection. NIH 3T3 cells were seeded into 6-well Costar plates at a concentration of 5×10^5 cells per well. Cells were infected by adding the specified virus to a concentration of 10^7 PFU/ml (MOI of 20 PFU/cell) without replacement of the medium. At the indicated times before or after infection, IFN-β was added directly to the medium to a concentration of 50 U/ml. After infection, medium was not replaced in any well. The released viruses were harvested at 20 h postinfection. To measure the titer of the residual infectious virus, virus sample was incubated for 20 h in the medium in the absence of cell monolayer. The arrow indicates the start of infection.

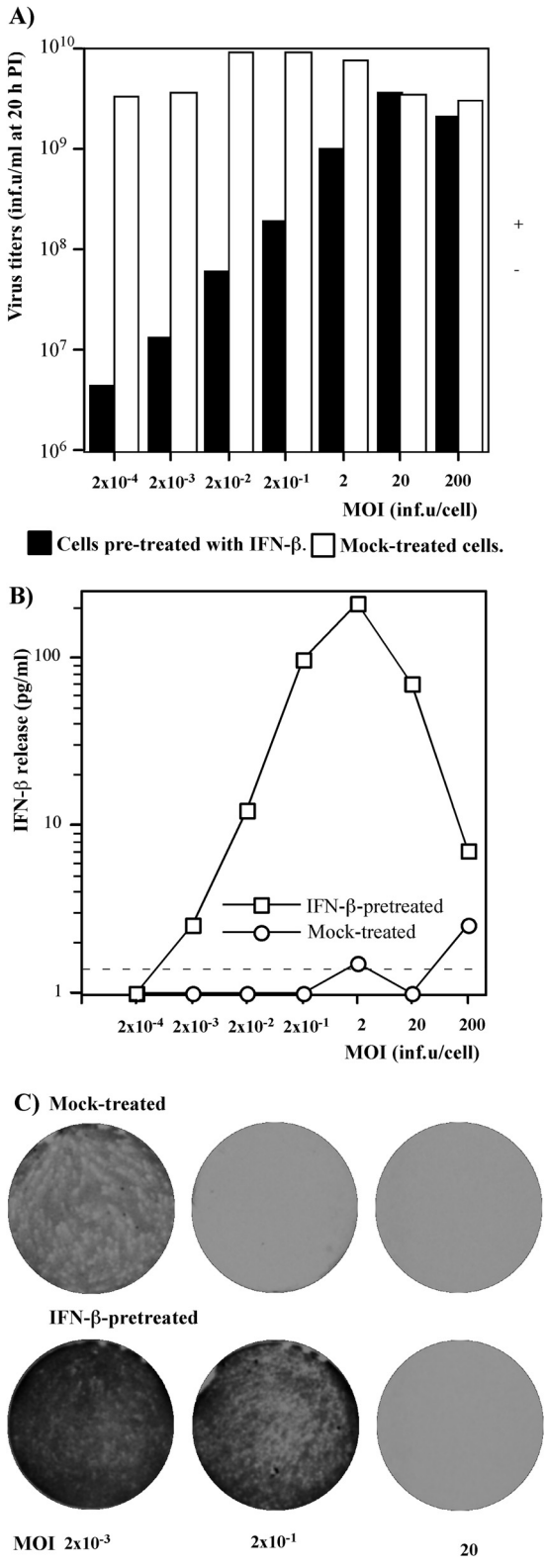

FIG 8 SINV replication, IFN-β release, and CPE development strongly depend on pretreatment of the cells with low doses of IFN-β. NIH 3T3 cells were seeded into 6-well Costar plates at a concentration of 5×10^5 cells per well. At 2 h before infection with SINV/GFP, IFN-β was added to some plates to a concentration of 0.2 U/ml, and then cells were infected at the indicated MOIs. In parallel, NIH 3T3 cells were infected at the same MOIs without IFN pretreatment. Samples were harvested at 20 h postinfection to measure virus release (A) and IFN-β concentration (B), and cells were stained with crystal violet to assess CPE development (C). The dashed line in panel B indicates the detection limit. The experiment was repeated 3 times and generated very reproducible data. The results of one of the experiments are presented.

the concentration of infecting virus is at biologically relevant levels, below 10^7 PFU/ml, which corresponds to the average levels of viremia.

DISCUSSION

One of the hallmarks of alphavirus infection in vertebrate hosts is development of high-titer viremia, which is required for virus transmission to mosquito vectors during their blood meal. At the same time, most of the alphaviruses induce both type I and type II interferon responses, which are aimed at downregulation of virus replication in infected and as-yet-uninfected cells and tissues. Viremia development and IFN induction are two competing processes, and so far, their relationships during alphavirus replication are not completely understood. This situation is particularly true in the case of SINV infection. This virus is known to be very sensitive to type I IFN treatment, and it is unclear how it can develop viremia in the presence of IFN-α/β concentrations approaching thousands of units per milliliter (12, 31, 40). In the case of VEEV infection, IFN-α/β accumulates to an even higher concentration that greatly exceeds the upper limit of virus resistance to type I IFN (31). It is also unclear how replication of alphaviruses, which have developed very efficient means of preventing IFN induction and activation of the other antiviral genes, remain able to induce type I and II IFNs *in vivo* with great efficiency. In this study, we made an attempt to provide plausible answers for at least some of these questions.

First, we hypothesized that the first rounds of replication of a small number of infectious SINV virions entering the cells play a critical role in the outcome of the infection. These cells not only produce infectious SINV for the next rounds of replication but also release low levels of cytokines and, importantly, type I IFN. This IFN release is determined by both the efficiency of virus replication in these cells and the ability of the virus to interfere with antiviral response development. We have readily detected a low level of IFN-β release from SINV-infected murine bone marrow cells and dendritic cells. Type I IFN has also been found to be released from SINV-infected human fibroblasts (44) and L929 cells infected by another SINV strain (7).

Our data demonstrate that the presence of IFN-β even at very low, subprotective concentrations, which are undetectable by standard biological IFN assay or ELISA, have a strong effect on SINV replication and infection spread. Cells pretreated with such low doses of IFN for a short period of time can still be productively infected and support virus replication. However, they respond to replicating virus by dramatically more efficient type I IFN expression and a higher level of ISG activation (Fig. 10). The newly released IFN can either protect the uninfected cells or perform further rounds of more efficient priming. Activation of IFN-β and ISG expression by low doses of IFN and virus replication suggests that IFN priming is likely a complex event, at least partially mediated by earlier and/or more efficient activation of IFN regulator factor 7 (IRF7) and/or IRF9. This in turn results in activation of the IFN-β promoter before development of transcriptional shutoff in the infected cells. Activation of ISGs is usually achieved

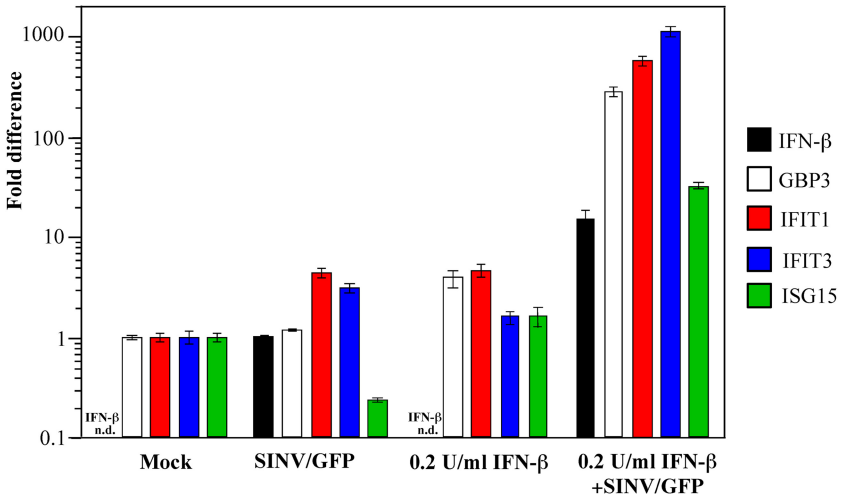

FIG 9 Pretreatment of NIH 3T3 cells with a low dose of IFN-β prior to SINV/GFP infection leads to higher levels of ISG induction. Total RNA was isolated from (i) naïve NIH 3T3 cells, (ii) cells treated with 0.2 U/ml of IFN-β for 20 h, (iii) cells infected with SINV/GFP at an MOI of 2 PFU/cell for 20 h, or (iv) cells pretreated with 0.2 U/ml of IFN-β for 2 h and then infected with SINV/GFP at 2 PFU/cell for 20 h. The data were normalized to the mean C_T of 18S RNA in each sample. The fold difference was calculated using the $\Delta\Delta C_T$ method, which uses the mean C_T of a mock-infected sample for normalization. The mRNA of IFN-β was not detected in the mock-infected or the IFN-β-treated (0.2 U/ml) samples. These data were normalized to the mean C_T in the virus-infected cells. The reactions were performed in triplicate, the data are presented as mean values, and standard deviations were calculated.

through the Jak-STAT/IRF9 pathway after binding of released type I IFN to the IFN-α/β receptor. However, this appears not to be the only means of ISG induction, because knockout MEFs lacking the IFN-α/β receptor can induce nearly the same spectrum of ISGs in response to replication of SINV/G/GFP and VEEV/Cmut/GFP as do wt MEFs (unpublished data). This is a very strong indication that they can be activated through a different pathway(s), which is yet to be identified. The presented data suggest that this pathway is also partially activated by IFN priming and further induced by virus infection. Its induction appears to stimulate IFN-β release and slower CPE development during SINV replication, which was detected in this study (Fig. 8C).

Thus, the previously described effects of differences in glycosylation of alphavirus glycoproteins on the ability of the virus to induce type I IFN (32) could have a strong effect on IFN induction in the first round(s) of replication. It has been shown that the Ross River virus, bearing envelope glycoproteins synthesized in mosquito cells, is a less efficient IFN inducer (32). It remains to be ascertained whether this could be a biologically significant phenomenon, because in natural alphavirus circulation only 10 to 100 infectious virions are transmitted to the host during a mosquito blood meal (36). It is difficult to understand how such a small number of virions with a mosquito-derived envelope could have a strong effect on the outcome of the infection. *In vivo*, infection proceeds through multiple rounds of replication and, thus, is mediated by virus progeny with envelope proteins already synthesized and glycosylated in the host cells. Our data suggest that the small number of viral particles delivered by a mosquito bite could be less efficient in IFN induction upon infection of the host cell. This, in turn, might be a reason for the further shift in the balance between viremia development and IFN induction from priming and type I IFN activation to higher viremia.

There is likely a very delicate cell-specific balance between SINV replication and activation of the antiviral response in cells infected during the first round of infection. Small changes in the virus's ability to inhibit cellular transcription, caused by specific mutations in the nsP2 protein, lead to dramatic changes in this balance. By 4 h postinfection, cells infected by efficiently replicating SINV nsP2 mutants, such as SINV/G/GFP or SINV/2V/GFP, do respond with high levels of IFN release. This leads to an inefficient spread of infection and an inability to infect all of the normally permissive, IFN-competent cells at a low MOI. Such mutants are no longer able to form plaques or foci of infected cells, but they still demonstrate efficient replication at high MOIs.

The negative effect of mutations in virus-specific proteins with nuclear functions appears not to be limited to SINV nsP2. VEEV TC-83 variants, containing mutations in the H68 peptide of capsid protein, which determines inhibition of nuclear cytoplasmic trafficking (3, 4), also induce a more efficient and earlier type I IFN induction (Fig. 2). It has been demonstrated that the New World alphavirus variants with mutations in this peptide, or encoding its homolog derived from the Old World alphaviruses, are highly attenuated *in vivo* (1, 17, 41). Thus, the nuclear functions of nsP2 and capsid proteins, which result in downregulation of the antiviral response, play an indispensable role in alphavirus pathogenesis and its ability to develop spreading infection.

The experimental data also suggest that it is unlikely that the type I IFN released due to viral infection has a robust or immediate effect on virus replication in already-infected cells. At 2 h postinfection, IFN-β treatment of the NIH 3T3 cells no longer had a detectable negative effect on established SINV replication. This resistance to IFN treatment occurs before the infection strongly affects phosphorylation of STAT1 or its intracellular concentration (35). This certainly does not rule out the possibility that changes in murine STAT1 phosphorylation and signaling are not involved in resistance of SINV replication to IFN-α/β treatment. However, the data do suggest that the disruption of Jak/STAT signaling takes place late, during the stage with the most efficient SINV release.

Thus, the results of our study demonstrate that the first few

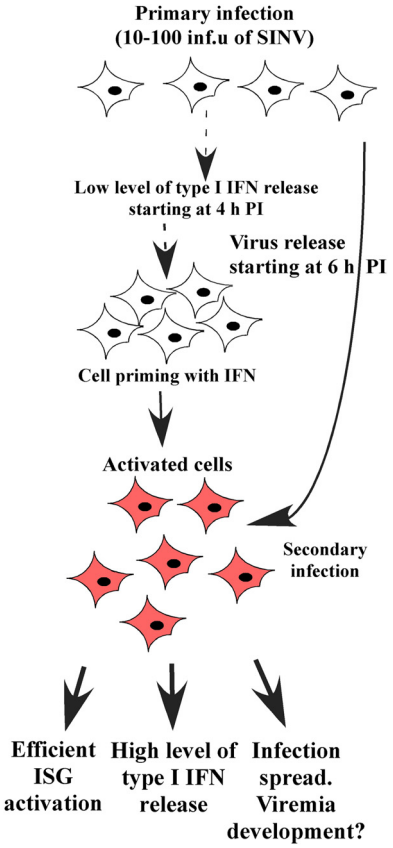

FIG 10 Schematic representation of the proposed mechanism of type I IFN and virus release in host cells infected with SINV. After the mosquito blood meal, a small dose of transmitted virus is sufficient for infection of approximately 10 to 100 cells. Starting from 4 h postinfection, infected cells release a very small, subprotective amount of type I IFN, and from 6 to 8 h postinfection, they begin virus production. The released IFN primes yet-uninfected cells, and upon subsequent rounds of infection with the released virus they not only produce virus but also respond with type I IFN expression levels that are orders of magnitude higher and more efficiently activate the antiviral response, which is undetectable without IFN priming. Thus, the natural infection leads to establishment of a balance between infection spread and innate immune response development. The first rounds of virus replication strongly depend on the integrity of virus-specific genes, the efficiency of virus replication in host cells, and the ability of the host to respond on a cellular level to virus replication.

hours of SINV replication play a critical role in infection development and spread. This initial period appears to determine the balance between type I IFN induction and the ability of the virus to produce the next rounds of infection (Fig. 10). Moreover, the experiments undertaken with VEEV TC-83 also suggest that the establishment of this balance is critical not only for SINV but for other alphaviruses as well.

Previously published studies have shown that the alphaviruses utilize numerous strategies to overcome the IFN response and develop more efficient replication. Some of the alphaviruses (the best example being eastern equine encephalitis virus) are poor IFN-α/β inducers (13), whereas some of them, such as VEEV, are more resistant to type I IFN (43). Others, such as SINV, appear to find a compromise between IFN induction and virus replication.

ACKNOWLEDGMENTS

This work was supported by Public Health Service grants AI070207, R56AI091705, and R01AI073301.

REFERENCES

1. **Aguilar PV, Leung LW, Wang E, Weaver SC, Basler CF.** 2008. A five-amino-acid deletion of the eastern equine encephalitis virus capsid protein attenuates replication in mammalian systems but not in mosquito cells. J. Virol. **82**:6972–6983.
2. **Aguilar PV, Weaver SC, Basler CF.** 2007. Capsid protein of eastern equine encephalitis virus inhibits host cell gene expression. J. Virol. **81**: 3866–3876.
3. **Atasheva S, Fish A, Fornerod M, Frolova EI.** 2010. Venezuelan equine encephalitis virus capsid protein forms a tetrameric complex with CRM1 and importin alpha/beta that obstructs nuclear pore complex function. J. Virol. **84**:4158–4171.
4. **Atasheva S, Garmashova N, Frolov I, Frolova E.** 2008. Venezuelan equine encephalitis virus capsid protein inhibits nuclear import in mammalian but not in mosquito cells. J. Virol. **82**:4028–4041.
5. **Atasheva S, Krendelchtchikova V, Liopo A, Frolova E, Frolov I.** 2010. Interplay of acute and persistent infections caused by Venezuelan equine encephalitis virus encoding mutated capsid protein. J. Virol. **84**:10004–10015.
6. **Burke CW, Gardner CL, Steffan JJ, Ryman KD, Klimstra WB.** 2009. Characteristics of alpha/beta interferon induction after infection of murine fibroblasts with wild-type and mutant alphaviruses. Virology **395**: 121–132.
7. **Cruz CC, et al.** 2010. Modulation of type I IFN induction by a virulence determinant within the alphavirus nsP1 protein. Virology **399**:1–10.
8. **Fazakerley JK, Boyd A, Mikkola ML, Kaariainen L.** 2002. A single amino acid change in the nuclear localization sequence of the nsP2 protein affects the neurovirulence of Semliki Forest virus. J. Virol. **76**:392–396.
9. **Frolov I, Garmashova N, Atasheva S, Frolova EI.** 2009. Random insertion mutagenesis of sindbis virus nonstructural protein 2 and selection of variants incapable of downregulating cellular transcription. J. Virol. **83**: 9031–9044.
10. **Frolov I, Schlesinger S.** 1996. Translation of Sindbis virus mRNA: analysis of sequences downstream of the initiating AUG codon that enhance translation. J. Virol. **70**:1182–1190.
11. **Frolov I, Schlesinger S.** 1994. Translation of Sindbis virus mRNA: effects of sequences downstream of the initiating codon. J. Virol. **68**:8111–8117.
12. **Frolova EI, et al.** 2002. Roles of nonstructural protein nsP2 and alpha/beta interferons in determining the outcome of Sindbis virus infection. J. Virol. **76**:11254–11264.
13. **Gardner CL, et al.** 2008. Eastern and Venezuelan equine encephalitis viruses differ in their ability to infect dendritic cells and macrophages: impact of altered cell tropism on pathogenesis. J. Virol. **82**:10634–10646.
14. **Gardner CL, Yin J, Burke CW, Klimstra WB, Ryman KD.** 2009. Type I interferon induction is correlated with attenuation of a South American eastern equine encephalitis virus strain in mice. Virology **390**:338–347.
15. **Garmashova N, et al.** 2007. Analysis of Venezuelan equine encephalitis virus capsid protein function in the inhibition of cellular transcription. J. Virol. **81**:13552–13565.
16. **Garmashova N, Gorchakov R, Frolova E, Frolov I.** 2006. Sindbis virus nonstructural protein nsP2 is cytotoxic and inhibits cellular transcription. J. Virol. **80**:5686–5696.
17. **Garmashova N, et al.** 2007. The Old World and New World alphaviruses use different virus-specific proteins for induction of transcriptional shutoff. J. Virol. **81**:2472–2484.
18. **Gorchakov R, Frolova E, Frolov I.** 2005. Inhibition of transcription and translation in Sindbis virus-infected cells. J. Virol. **79**:9397–9409.
19. **Gorchakov R, et al.** 2008. A new role for ns polyprotein cleavage in Sindbis virus replication. J. Virol. **82**:6218–6231.
20. **Gorchakov R, Frolova E, Williams BR, Rice CM, Frolov I.** 2004. PKR-dependent and -independent mechanisms are involved in translational shutoff during Sindbis virus infection. J. Virol. **78**:8455–8467.
21. **Griffin DE.** 1986. Alphavirus pathogenesis and immunity, p 209–250. *In* Schlesinger SS and Schlesinger MJ (ed), The *Togaviridae* and *Flaviviridae*. Plenum Press, New York, NY.
22. **Griffin DE.** 2001. Alphaviruses, p 917–962. *In* Knipe DM, Howley PM (ed), Fields virology, 4th ed. Lippincott, Williams and Wilkins, Baltimore, MD.

23. **Griffin DE.** 1989. Molecular pathogenesis of Sindbis virus encephalitis in experimental animals. Adv. Virus Res. **36**:255–271.
24. **Heise MT, Simpson DA, Johnston RE.** 2000. A single amino acid change in nsP1 attenuates neurovirulence of the Sindbis-group alphavirus SAAR86. J. Virol. **74**:4207–4213.
25. **Hidmark AS, et al.** 2005. Early alpha/beta interferon production by myeloid dendritic cells in response to UV-inactivated virus requires viral entry and interferon regulatory factor 3 but not MyD88. J. Virol. **79**: 10376–10385.
26. **Klimstra WB, et al.** 1999. Infection of neonatal mice with Sindbis virus results in a systemic inflammatory response syndrome. J. Virol. **73**:10387–10398.
27. **Lemm JA, Durbin RK, Stollar V, Rice CM.** 1990. Mutations which alter the level or structure of nsP4 can affect the efficiency of Sindbis virus replication in a host-dependent manner. J. Virol. **64**:3001–3011.
28. **Liljeström P, Lusa S, Huylebroeck D, Garoff H.** 1991. *In vitro* mutagenesis of a full-length cDNA clone of Semliki Forest virus: the small 6,000-molecular-weight membrane protein modulates virus release. J. Virol. **65**: 4107–4113.
29. **Rice CM, Levis R, Strauss JH, Huang HV.** 1987. Production of infectious RNA transcripts from Sindbis virus cDNA clones: mapping of lethal mutations, rescue of a temperature-sensitive marker, and *in vitro* mutagenesis to generate defined mutants. J. Virol. **61**:3809–3819.
30. **Rikkonen M, Peranen J, Kaariainen L.** 1992. Nuclear and nucleolar targeting signals of Semliki Forest virus nonstructural protein nsP2. Virology **189**:462–473.
31. **Ryman KD, Klimstra WB.** 2008. Host responses to alphavirus infection. Immunol. Rev. **225**:27–45.
32. **Shabman RS, Rogers KM, Heise MT.** 2008. Ross River virus envelope glycans contribute to type I interferon production in myeloid dendritic cells. J. Virol. **82**:12374–12383.
33. **Shirako Y, Strauss JH.** 1994. Regulation of Sindbis virus RNA replication: uncleaved P123 and nsP4 function in minus strand RNA synthesis whereas cleaved products from P123 are required for efficient plus strand RNA synthesis. J. Virol. **185**:1874–1885.
34. **Simmons JD, et al.** 2009. Venezuelan equine encephalitis virus disrupts STAT1 signaling by distinct mechanisms independent of host shutoff. J. Virol. **83**:10571–10581.
35. **Simmons JD, Wollish AC, Heise MT.** 2010. A determinant of Sindbis virus neurovirulence enables efficient disruption of Jak/STAT signaling. J. Virol. **84**:11429–11439.
36. **Smith DR, et al.** 2006. Venezuelan equine encephalitis virus transmission and effect on pathogenesis. Emerg. Infect. Dis. **12**:1190–1196.
37. **Strauss JH, Strauss EG.** 1994. The alphaviruses: gene expression, replication, evolution. Microbiol. Rev. **58**:491–562.
38. **Tesfay MZ, et al.** 2008. Alpha/beta interferon inhibits cap-dependent translation of viral but not cellular mRNA by a PKR-independent mechanism. J. Virol. **82**:2620–2630.
39. **Trgovcich J, Aronson JF, Johnston RE.** 1996. Fatal Sindbis virus infection of neonatal mice in the absence of encephalitis. Virology **224**:73–83.
40. **Trgovcich J, et al.** 1997. Sindbis virus infection of neonatal mice results in a severe stress response. Virology **227**:234–238.
41. **Wang E, Kim DY, Weaver SC, Frolov I.** 2011. Chimeric Chikungunya viruses are nonpathogenic in highly sensitive mouse models but efficiently induce a protective immune response. J. Virol. **85**:9249–9252.
42. **Weaver SC, Frolov I.** 2005. Togaviruses, p 1010–1024. *In* Mahy BWJ, ter Meulen V (ed), Virology, vol 2. Hodder Arnold, Salisbury, United Kingdom.
43. **White LJ, Wang JG, Davis NL, Johnston RE.** 2001. Role of alpha/beta interferon in Venezuelan equine encephalitis virus pathogenesis: effect of an attenuating mutation in the 5′ untranslated region. J. Virol. **75**:3706–3718.
44. **White LK, et al.** 2011. Chikungunya virus induces IPS-1-dependent innate immune activation and protein kinase R-independent translational shutoff. J. Virol. **85**:606–620.